國立臺灣大學生命科學院生命科學系

碩士論文

Department of Life Science

College of Life Science

National Taiwan University

Master Thesis

藍斑核活化後長抑制反應機制探討

Investigation of mechanisms underlying post-stimulation inhibition in locus coeruleus

詹鎬

Hao Chan

指導教授：閔明源 博士

Advisor: Ming-Yuan Min, Ph.D.

中華民國 111 年 7 月

July 2022

doi:10.6342/NTU202203169

國立臺灣大學碩士學位論文
口試委員會審定書

藍斑核活化後長抑制反應機制探討

Investigation of mechanisms underlying post-stimulation inhibition in Locus Coeruleus

本論文係詹鎬君（r09b21001）在國立臺灣大學生命科學學所完成之碩士學位論文，於民國 111 年 07 月 29 日承下列考試委員審查通過及口試及格，特此證明

口試委員：

（簽名）

（指導教授）

生命科學系 系主任 黃偉邦 （簽名）

doi:10.6342/NTU202203169

致謝

感謝閔老師的從我大三下進入實驗室以來的指導。在進行研究的過程中我時常因為一些旁枝末節的問題而開始鑽牛角尖陷入，感謝閔老師耐心的指導並給予許多實用的建議。感謝昭成學長、瑋辰學長、幸君學姊、戎建學長等所有曾經指導過我實驗進行的人們，從他們身上我學到了許多不同的技術與做實驗的方法。

doi:10.6342/NTU202203169

中文摘要

藍斑核為腦中主要正腎上腺素來源，參與如警覺、清醒睡眠等多種反應。藍斑核有著持續、低頻的 tonic activity 與短暫高頻的 phasic activity 兩種模式，在近年的研究中發現 phasic activity 可能參與意識轉移與優化行為表現等複雜認知功能。phasic activity 常常由伴隨著一段長時間的抑制(PSI)，可能扮演過濾外界雜訊的功能。關於 PSI 我們提出三種假說。首先，藍斑核可能釋放正腎上腺素活化自身抑制性 α_2 正腎上腺素受體來造成抑制。其次，藍斑核 phasic activity 可能活化 SK、BK 與 IK 等鈣活化鉀離子通道造成抑制。最後，藍斑核也可能透過以 phasic activity 刺激週邊抑制性中間神經元來達到對自身進行抑制的現象。實驗中，我們透過腦片電生理的方式紀錄人工誘發 phasic-like activity 並觀察其後的抑制現象。結果顯示自發 tonic activity 頻率與 PSI 持續時間呈現負相關。藥理測驗則顯示 α_2-正腎上腺素受體抑制劑 (idazoxan)、SK 通道抑制劑 (apamin) 與 $GABA_b$ 受體抑制劑 (cgp54626) 皆可縮短 PSI 持續時間，顯示 α_2-正腎上腺素受體、SK 通道與 $GABA_b$ 受體應皆有參與 PSI 的產生。

關鍵字: 藍斑核、正腎上腺素、抑制性中間神經元、鈣活化鉀離子通道、phasic 反應。

doi:10.6342/NTU202203169

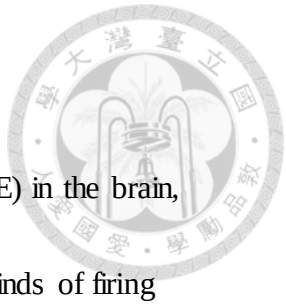

Abstract

Locus Coeruleus (LC) is the main source of Norepinephrine (NE) in the brain, involving in vigilance, arousal and wake sleep cycle. There are two kinds of firing pattern of LC, continuous low frequency tonic activity and brief high frequency phasic activity. Recent studies have shown that LC phasic activity may participate in complex cognitive function like cognitive shift and optimizing performance. Post stimulation inhibition (PSI) is often observed following phasic activity, which may benefit performance by filtering out distractions. We proposed three possible mechanisms of PSI. First, auto-releasing NE from LC neurons may bind to inhibitory α_2-adrenoreceptor (α_2-AR) causing PSI. Second, phasic activity may activate calcium-dependent potassium channel (SK, BK and IK channel) causing PSI. Last, LC phasic activity may stimulate surrounding inhibitory interneurons causing PSI. We conduct ex-vivo brain slice electrophysiology on LC neurons, and investigate in mechanism underlying inhibition following manually induced phasic like burst activity. We found that baseline spontaneous firing rate is negatively related to PSI duration, and that α_2-AR antagonist idazoxan, SK channel blocker apamin and GABAb receptor blocker cgp54626 could all reduce PSI duration, suggesting that α_2-AR, SK channel and GABAb receptor all take part in PSI.

doi:10.6342/NTU202203169

Key words : locus coeruleus, Norepinephrine, inhibitory interneuron, Calcium dependent potassium channel, phasic activity

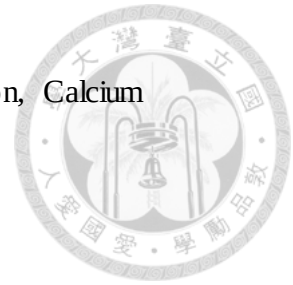

doi:10.6342/NTU202203169

Content

doi:10.6342/NTU202203169

doi:10.6342/NTU202203169

doi:10.6342/NTU202203169

Chapter 1. Introduction

1.1 Locus Coeruleus and Norepinephrine system

Locus Coeruleus (LC) consist of densely packed Norepinephrine (NE) neurons, located bilaterally in the dorsal pons and lateral to the 4th ventricle. LC axons project to spinal cord and nearly the whole brain (Schwarz et al. 2015, Plummer et al. 2020), serving as the major source of NE in the brain (Foote et al. 1987). LC axon terminals often form non-synaptic axonal varicosities which can release NE into extracellular space, affecting multiple neurons within certain region at once (Séguéla et al. 1990). LC-NE system is involved in a variety of behaviors, including vigilance, arousal, sleep-wake transition, behavioral adaptation…etc (Aston-Jones et al. 1981, Aston-Jones et al. 1994, Xiang et al. 2019).

The effects of NE on target neurons would be determined by the adrenoceptors (ARs) being activated. ARs are G-protein couple receptors and have several subtypes, including α_1, α_2, β_1, β_2, β_3(Zhong et al. 1999), each with different functions. For example, α_2 ARs are primary linked to G_i proteins (Ramos et al. 2006), and may increase potassium conductance (Zhao et al. 2008, Arima J et al. 1998), inhibiting Ca^{2+} channel (Timmons et al. 2004) and inhibiting hyperpolarization-activated cyclic nucleotide-gated channels (HCN) by suppressing cAMP formation (Marzo A et al. 2009,

doi:10.6342/NTU202203169

Ramos et al. 2006). On the contrary, α_1 ARs are generally coupled with G_q, and are capable of inducing intracellular Ca^{2+} release and decrease of K^+ conductance (Aghajanian et al. 1985, Marzo A et al. 2009). Since AR subtypes distribute differently in the brain (Scheinin et al. 1994, Pieribone et al. 1994), effects of LC-NE system can vary from region to region.

1.2 LC tonic and phasic activity

LC neurons can exhibit relative low frequency continuous discharging, called tonic activity which takes critical roles regulating cortical arousal levels (Aston-Jones et al 1981). LC tonic activity is nearly silence during REM sleep, and optogenetic stimulation in mice LC can cause transition from sleep to awake (Carter et al. 2010). LC neurons can also perform short latency high frequency (over 10 Hz) phasic activity which often observed following novel and salient stimuli, including nociceptive stimuli (Neves et al. 2018, Grella et al. 2019, Chen and Sara, 2007). LC neurons can also respond phasically to task related stimuli (Clayton et al. 2004). Take Go/No-Go task for instance, rats were trained to go to target region once onset cue was presented. The rats should then go to reward region after receiving positive cues, but not the distractors. In the experiments, phasic activity can be observed following onset cues and positive cues, but not distractors (Bouret and Sara, 2004). Other studies upon behavior task

doi:10.6342/NTU202203169

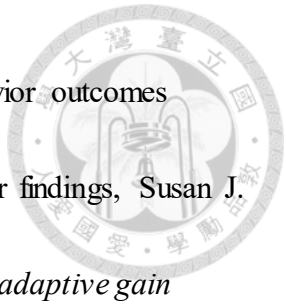

performance have also suggested roles of LC phasic activity on behavior outcomes (Rajkowski et al. 2004, Clayton et al. 2004). With this and many other findings, Susan J. Sara and Astone Jones have each proposed *Network reset theory* and *adaptive gain theory*, suggesting phasic activity in respond to target cue may take part in optimizing performance (Bouret and Sara, 2005, Astone-Jones and Jonathan D Cohen, 2005).

Recent studies have shown that LC phasic activity takes part in cortical response to salient sensory stimuli, and that LC phasic activation can reset familiar spatial map of hippocampus even in familiar environment (Vazey et al. 2018, Grella et al. 2019), exhibiting ability of LC phasic activity in reorganizing neural network. Tonic activity can also affect performance. At high frequency of LC tonic activity, animals are more active but also more distractible. Study has shown that during elevated tonic firing rate, animals prone to respond to stimuli (targets or distractors) more, with reduced accuracy (Aston-Jones et al. 1994).

1.3 Post stimulation inhibition (PSI)

Long lasting inhibition on tonic rate is often observed post LC phasic activation (Chen and Sara, 2007, Astone Jones et al. 1994, Jodo et al. 1998). We refer the phenomenon as post stimulation inhibition (PSI). As mentioned above, high frequency LC tonic activity can cause more activity with lower accuracy (Aston-Jones et al. 1994).

doi:10.6342/NTU202203169

On the contrary, during PSI, inhibition on tonic activity could makes subject less active and less distractible, which may as well optimize performance. In Go/No-Go task, PSI can be observed following phasic activity evoked by onset cue (Bouret and Sara, 2004), which could benefit the subject in expecting for odor cues by filtering out environmental distractions. Moreover, PSI can also be observed following in-vivo antidromic or intracellular rat LC stimulation (Ennis and Aston-Jones, 1986, Aghajanian et al. 1982). The fact that intracellular stimulation can still generate PSI suggests it should be caused by intrinsic property of LC neurons or local circuits without involvement of other brain nucleuses.

1.4 Possible mechanisms underlying post stimulation inhibition (PSI)

According to previous studies, we proposed three possible mechanisms underlying PSI generation. First, α_2-adrenoceptor (α_2-AR) has been found on LC neurons, and thus applying NE and α_2-AR agonist could both decrease LC neurons spontaneous firing frequency (Cedarbaum et al. 1976, Jedema et al. 2008). LC neurons have shown capability of releasing NE from somatodendritic site, leading to auto-inhibition by α_2-ARs and producing negative-feedback (Huang et al. 2012) It is possible that NE released during LC phasic activity may bind to their own α_2-ARs and cause PSI. In addition, Norepinephrine mediate lateral inhibition can also be observed between LC

doi:10.6342/NTU202203169

neurons (Aghajanian et al. 1977, Ennis and Aston-Jones, 1986); as a result, LC neurons generating phasic activity together could also contribute to PSI of each other through α_2-AR.

Second, intrinsic properties of LC neurons may also contribute to PSI. Voltage dependent calcium channels (Cav channels) open following action potential (AP). Cav channels like T and L-type Ca^{2+} channels have been observed in LC neurons, and involve in the regulation of spontaneous activity (Matschke et al. 2015). Ca^{2+} dependent K^+ (K_{Ca}) current which involves in the prolonged afterhyperpolarization (AHP) are also observed in LC neurons (Andrade and Aghajanian, 1984). As a result, LC neurons phasic activities could activate Cav channels, causing Ca^{2+} influx. Ca^{2+} influx could then stimulate K_{Ca} channels and generate PSI. There are three main subtypes of K_{Ca} channels, small conductance (SK), intermediate conductance (IK) and big conductance channels(BK) (Stocker et al. 2004, Sah et al. 2002). All three channels have been reported in LC neurons (Matschke et al. 2018, Kawano et al. 2020).

Third, GABAergic inhibitory interneurons can be found around LC region like peri-LC dendritic zone (Aston-Jones et al. 2004). If excitatory ARs like α1-ARs are expressed in inhibitory interneurons forming contacts with LC neurons, NE released from somatodendritic site and axons during phasic activity could activate these inhibitory interneurons, and contribute to PSI.

doi:10.6342/NTU202203169

1.5 Aim of this study

Our experiments showed that PSI could also be observed after burst of Aps induced by injecting depolarizing current into LC neurons using acute brain slices. We aim to use this as a model to further investigate in all three possible mechanisms underlying PSI.

doi:10.6342/NTU202203169

Chapter 2. Material and methods

2.1 Animals

All experiments were conducted with C57BL/6 mice which were descendants of Th-cre mice cross bred with Ai32 mice (TH-cre x Ai32). Both mice were obtained from Jax Lab (Stock #: 00861 and 024109). Animal welfare was supervised by Institutional Animal Care and Use Committee IACUC) of National Taiwan University. Th-cre mice express cre recombinase on Tyrosine hydroxylase positive neurons, including LC neurons. Neurons of Ai32 mice would express channelrhodopsin 2 (chr2) in the presence of cre recombinase. Altogether, Th-cre x Ai32 mice could express chr2 in LC neurons, hence can be stimulated by blue light.

2.2 Acute brain slices preparation

NMDG protective recovery method were adopted to prepare acute brain slices (Ting et al. 2014). To start, an adult Th-cre x Ai32 mouse was anaesthetized in a container with 200 μL isoflurane, following intraperitoneal urethane 1.3 g/ 1 kg injection. After checking the absence of pain reflex by pinching digits with a tweezer, the mouse was perfused with 10 mL cold NMDG-aCSF which contains (in mM) : N-Methyl-D-glucamine 92, KCl 2.5, NaH_2PO_4 1.25, $NaHCO_3$ 30, HEPES 20, Glucose 25,

doi:10.6342/NTU202203169

$MgSO_4$ 10, $CaCl_2$ 0.5, sodium ascorbate 5, sodium pyruvate 3, adjusting to 315-318 mOsm by sucrose and to ph 7.35-7.38 by NaOH and HCl. The brain was dissected out, and then cutting into 350 μm thick coronal slices in cold NMDG-HEPES-aCSF using a vibratome (Leica VT 1000s), and slices containing LC neurons were collected. The brain slices were then incubated in 35°C NMDG-aCSF for 30 mins, and then mixed in same volume of HEPES-aCSF which contains (in mM) : NaCl 92, KCl 2.5, NaH_2PO_4 1.25, $NaHCO_3$ 30, HEPES 20,Glucose 25, $MgSO_4$ 2, $CaCl_2$ 2, sodium ascorbate 5, sodium pyruvate 3, adjusting to 310-313 mOsm by sucrose and to ph 7.35-7.38 by NMDG and HCl, and incubate again for 25 mins. Next, the brain slices was transferred in HEPES-aCSF and rest for at least 45 mins until electrophysiologic experiments. During recording, slices will be continuously perfused with aCSF which contains (in mM) : NaCl 119, KCl 2.5, NaH_2PO_4 1, $NaHCO_3$ 26.2, Glucose 11, $MgSO_4$ 1.3, $CaCl_2$ 2.5, adjusting to 315-308 mOsm by sucrose and to ph 7.35-7.38 by NaOH and HCl. All buffers should be bubbled with 95% O_2, 5% CO_2 before and during usage.

2.3 Electrophysiologic experiments

For each experiment, a brain slice was placed in the recording chamber on an upright microscope, and continuously perfused with aCSF (2-3 mL / min) bubbled with

doi:10.6342/NTU202203169

95% O_2 and 5% CO_2. Images were obtained with a Differential Interference Contrast (DIC) optic system (BX51WI, Olympus Optical Co.) and a CCD camera (ORCA-R2, Hamamatsu Photonics). Glass pipettes (tip resistance of 10-15 MΩ) were pulled from borosilicate glass capillaries (GC150F-10, Warner Instruments) using pipette puller (PC-100, Narishige). For whole-cell patch-clamp recording, glass pipettes were filled with K-glu internal buffer containing (in mM): EGTA 2, K-Gluconate 131, HEPES 10, KCl 2, NaCl 8, ATP 2, GTP 0.3, biocytin 33.56, adjusting to 300-305 mOsm by sucrose, adjusting to 7.2-7.25 pH by KOH. In current-clamp, action potentials must overshoot 0 mV for the data to be accepted. In voltage-clamp, membrane potential would be clamped at -70 mV unless otherwise specified, and serial resistance variation should remain within 20% from origin value. For cell-attach recording, glass pipettes were filled with aCSF, and current-clamp mode would be used. Recording signals was amplified with Multiclamp 700B amplifier (Moliecular Device), and a 2 kHz low-pass filter would be applied. It was then digitalized at 10 kHz with Micro 1401 (Cambridge Electronic Design).

2.4 PSI duration measurement

To measure poststimulation inhibition (PSI) duration, whole-cell current-clamp or cell-attach recording were conducted from LC neurons, and recordings were cut into 20

doi:10.6342/NTU202203169

seconds long trials. At 5 sec post initiation in every trial, a burst activity of 4 APs around 12 hz were evoked by either current injection of four 10 ms square pulses (increasing intensity of each from 250 pA until capable of generating AP), or optogenetically stimulated by of four 470 nm 10 mW/cm^2 light pulses (increasing latency from 2ms until capable of generating AP). During experiments if the neuron failed to generate 4 APs several times in a row, the intensity of stimulation would be adjusted till the point when burst activities were successfully generated again. The light pulses were generated by a LED OptoLED light source (Cairn Research) triggered by Micro 1401.

After collecting at least 50 trials, we would select frames that successfully generate 4 APs burst and without spontaneous phasic activity interfering PSI, and take the average value of duration between the last AP of induced burst activities and the first following spontaneous AP as PSI duration. Baseline activities were defined as average AP number before stimulation divided by latency of Baseline period (Hz). Throughout recordings, baseline activity would be monitored and maintained around the same frequency by adjusting holding current right before trial initiation. Burst frequency were calculated by averaging inverse burst AP intervals (1/interval).

doi:10.6342/NTU202203169

2.5 Optogenetic induced outward current

To test the outward current observed following optogenetic stimulation, we conduct whole cell voltage clamp on LC neurons with voltage clamped at either -40 mV or -50 mV, and optogenetically stimulate the neuron with a train of light pulses (470 nm, 10 mW/cm^2, 2ms) every 20 seconds to observe the outward current following stimulation.

2.6 Immunohistochemistry (IHC) staining

For post hoc validation of electrophysiologic brain slices, brain slices were fixed with paraformaldehyde right after experiments for at least one night. To stain TH and biocytin (labeling whole-cell patch LC neurons), the brain slices were first washed with 0.1 M phosphate buffer (0.1 M PB) for 5 min 3 times. The slices were then placed in blocking solution (0.2% bovine serum albumin (BSA) in phosphate buffered saline with 0.3% Triton X-100 (PBST)) and shaken for 1 hour under room temperature, followed by transferring to 1st antibody solution containing 1:1000 dilution of rabbit anti-TH (AB152 Merck Millipore) in PBST and shaken overnight at 4°C. Brain slices were next been washed with 0.1 M PB for 5 min 3 times, afterward, they were shaken for 2 hours in a mixture of 2nd antibodies containing 1:200 dilution of goat anti-rabbit conjugated Alexa Fluor 594 and 1:200 dilution of streptavidin conjugated Alexa Fluor

doi:10.6342/NTU202203169

405 (Jackson Immuno Research) in PBST under room temperature. In the mixture, streptavidin can bind to biocytin, hence staining biocytin labeled neurons. Finally, the brain slices were again washed with 0.1 M PB, before mounted with Rapiclear mounting solution (SunJin Lab) and examined with a Zeiss LSM 780 confocal microscopic system (Carl Zeiss).

2.7 Data analysis

Data were analyzed with R studio, Excel and Prism 8. To compare data before and after drug application, normality was first tested using the Shapiro-Wilk test. If all groups showed normal distribution, paired t test were used. If not, non-parametric paired Wilcoxon-sign rank test would be used instead. $P < 0.05$ were noted as *, $p < 0.01$ as ** and $p < 0.001$ as ***. Data were presented as mean ± SD.

doi:10.6342/NTU202203169

Chapter 3. Result

To test possible mechanisms underlying PSI, whole-cell current-clamp recordings were conducted on LC neurons using acute brain slices (Fig.1 A). As shown in Fig.1 B, burst activities composed of 4 APs around 12 Hz were evoked by injecting depolarizing current (I-injection). Mean latencies between last AP of burst activity and next spontaneous AP were measured and defined as post-stimulation inhibition (PSI) durations. Mean values of how many spontaneous APs occurred per second before stimulation (Fig.1 B blue line) were defined as baseline activities, and mean inter spike interval of baseline was defined as baseline spike interval. Our internal solution contained biocytin. After experiments brain slices would be fixed and stained TH and biocytin for post hoc validation (Fig.1 C).

3.1 Baseline activity and PSI duration

Previous study has shown that burst frequency and AP number would affect PSI duration (Andrade and Aghajanian, 1984). However, the effects of baseline activity on PSI duration has not been studied. As shown in Fig.2 A, we examined PSI evoked with different levels of baseline activity, which was controlled to around 1, 2, 4, 8 Hz by adjusting the holding current intensities. As shown in Fig2. B1, PSI durations for baseline activity around 1 ,2 ,4, 8 Hz were (in sec) 2.2 ± 0.12, 0.92 ± 0.04, 0.37 ±0.02

doi:10.6342/NTU202203169

and 0.14 ± 0.002 respectively (n = 7, $p < 0.0001$ for 1, 2 Hz, $p < 0.0001$ for 2, 4 Hz, $p = 0.0002$ for 4, 8 Hz). The relationships of PSI duration with baseline activity and baseline spike interval were shown in Fig2. B. As shown in Fig11. A1, Linear regression test indicated that baseline spike interval and PSI duration has a linear relationship that can be described by following equation $y = 2.3875x – 0.233$ with $R^2 = 0.9621$, where x is baseline spike interval and y is PSI duration. As shown in Fig.11 A2, when pooling all whole-cell recorded data before pharmacology treatment in all following experiments, the same linear relationship can still be observed ($y = 2.5869x – 0.366$, $R^2 = 0.9417$). These results indicated that PSI duration would be affected by baseline activity, hence maintaining similar baseline activity throughout recording is important for PSI duration measurement. As a result, in the following experiments, we would maintain baseline activity by adjusting holding current at similar level throughout the experiments.

3.2 PSI duration of optogenetic and I-injection induced burst

Study has shown that antidromic stimulation on LC neurons through midbrain dorsal noradrenergic bundle would still generate inhibition on tonic activity even when stimulation was not strong enough to driven burst activity on recorded neurons, suggesting that inhibition should exist between LC neurons (Ennis et al. 1986). Our

doi:10.6342/NTU202203169

experiments also showed similar result. While applying optogenetic stimulation, some neurons failed to generate burst activity, which were referred as non-driven neurons. As shown in Fig.3 A, we recorded non-driven neurons and applied light stimulation every other trail, and then measured spike interval between last AP within stimulation period and the next spontaneous AP. The results were presented in Fig.3 B, we could find that spike intervals of non-driven neurons with light stimulation were significantly longer than those without light stimulation. Spike intervals with and without light stimulation of non-driven neurons were : 1.62 ± 0.13 sec and 1.08 ± 0.05 sec ($p = 0.0089$, $n = 6$). Also shown in Fig.3 B, spike intervals of non-driven neurons with light stimulation were significantly shorter than PSI durations of driven neurons (2.71 ± 0.18 sec, unpaired t-test : $p = 0.0006$, $n = 7$). The result indicated that optogenetic stimulation could still generate inhibition in the absence of burst activity. Since light stimulation would also be applied to non-recording neurons, the Inhibition may be caused by inhibition from other LC neurons that successfully generated burst activity.

As a result, we would like to know whether PSI following optogenetic stimulation (stimulating all neurons expressing chr2) would differ from inhibition following I-injection (stimulating only recorded neuron). Namely, whether other LC neurons fire burst activities simultaneously would contribute to PSI duration through inhibition between each other. To test this theory, as shown in Fig.4 A (upper half), we alternately

doi:10.6342/NTU202203169

used optogenetic stimulation and I-injection to induce burst activities, and measured PSI durations for optogenetic stimulation and I-injection. PSI duration for optogenetic stimulation was 2.34 ± 0.25 and PSI duration for I-injection was 2.36 ± 0.18 sec (n = 7, p = 0.9006). As shown in Fig.4 B(left half), PSI durations were not significantly different between optogenetic stimulation and I-injection, suggesting inhibition between LC neurons may not contribute to PSI duration. Since no significance different between optogenetic stimulation and I-injection induced PSI duration was observed, unless otherwise specified, we would only use I-injection in the following experiments.

3.3 Effects of α_2-AR on PSI : idazoxan decrease PSI duration

Since applying NE on LC neurons can cause inhibition on tonic rate, and the degree of inhibition can be significantly reduced in the presence of α_2-AR antagonist (Cedarbaum et al. 1976), α_2-AR could contribute to PSI. To test this theory, 10 μM idazoxan, an α_2-AR antagonist, was applied (Fig.4 A). As shown in Fig.4 B, PSI durations were significantly decreased after idazoxan application. PSI durations following optogenetic induced burst activities before and after idazoxan application were 2.34 ± 0.25 and 1.97 ± 0.24 (n = 7, p = 0.0074). PSI durations following I-injection induced burst activities before and after idazoxan application were 2.36 ± 0.18 and 2.22 ± 0.18 (n = 7, p = 0.0282). The result indicates that α_2-AR should contribute to

doi:10.6342/NTU202203169

PSI. Since baseline activity and burst frequency remained unchanged for both optogenetic stimulation and I-injection (Fig.4 C), effects of idazoxan on PSI duration should be independent of baseline activity.

In addition, as presented in Fig.5 A, outward currents could be observed following optogenetic stimulation in some LC neurons (15/43). As shown in Fig.5 B and C, the current could be partially inhibited by idazoxan. Amplitude before and after idazoxan (in pA) : 4.70 ± 0.71 and 3.94 ± 0.55 ($p = 0.0098$, $n = 10$), charge transfer before and after idazoxan (in pC) : 3.88 ± 0.92 and 1.95 ± 0.54 ($p = 0.0020$, $n = 10$). The result indicate that α_2-AR was activated following optogenetic stimulation, and that α_2-AR was not the only component of the outward current.

3.4 Effects of extracellular calcium concentration on PSI

Since K_{Ca} current following evoked burst activity has been reported in LC neurons (Andrade, R, and G K Aghajanian, 1984), K_{Ca} channels could also contribute to PSI. But before testing effects of K_{Ca} channels on PSI, we would like to check the effects of extracellular calcium concentration on PSI duration. In the experiments, as presented in Fig.6 A, we applied 0.2 mM calcium aCSF then washing back to normal aCSF (2.5 mM calcium). As presented in Fig 6. B, PSI durations were significantly decreased when aCSF calcium concentration was changed from 2.5 mM to 0.2 mM. The PSI durations

doi:10.6342/NTU202203169

for aCSF, 0.2 mM aCSF and wash (aCSF) were 0.98 ± 0.04, 0.84 ± 0.02 and 0.94 ± 0.06 seconds (n = 9, p = 0.0037 for aCSF and 0.2 mM calcium aCSF, p = 0.1138 for 0.2 mM calcium aCSF and wash).

However, since LC neurons tonic activity would keep rising in 0.2 mM calcium aCSF, despite trying to maintain baseline activities by adjusting holding current, baseline activities still accelerated (1.94 ± 0.04 to 2.16 ± 0.03 Hz, p = 0.006). As mentioned above, since baseline activity has accelerated, it could also contribute to the decrease of PSI duration. As shown in Fig.6 C, we can also see that burst frequency slightly increased in 0.2 mM calcium aCSF. However, according to Fig.11 B, these small changes in burst activity should not cause much difference in PSI duration.

3.5 Effects of K_{Ca} channels on PSI : apamin decrease PSI duration

3.5.1 Whole-cell recording with 2 mM EGTA internal buffer

To test the effects of K_{Ca} channels on PSI duration, we applied blockers for three main K_{Ca} channels including 0.2 μM apamin for SK channel, 10 μM paxilline for BK channel and 10 μM TRAM 34 for IK channel (Fig.7 A). As presented in Fig.7 B and C, all three K_{Ca} blockers had no significant effect on PSI duration, baseline activity and burst frequency. PSI durations before and after K_{Ca} blockers were (in sec) apamin : 0.99 ± 0.04 and 0.95 ± 0.04 (n = 8, p = 0.0906), paxilline : 0.93 ± 0.04 and 0.92 ± 0.06 (n =

doi:10.6342/NTU202203169

8, p = 0.3828), TRAM 34 : 0.93±0.03 and 0.95 ± 0.03 (n = 7, p = 0.5372).

3.5.2 Extracellular attach recording

While conducting whole-cell patch, EGTA, a calcium chelator, is often added in internal solution to stabilize intracellular calcium concentration. However, study has shown that intracellular EGTA could affect SK channel (Matschke et al. 2018). It is possible that K_{Ca} channel blockers had no obvious effects on PSI was due to EGTA (2 mM) in internal solution.

To address this problem, we repeated same experiments, but using cell-attach recording and optogenetic stimulation this time (Fig.8 A and B). Since there would be no contact between internal solution and cytoplasm, intracellular calcium concentration should not be affected. As shown in Fig. 8 C and D, PSI durations were only significantly decreased after apamin application. PSI durations before and after K_{Ca} channel blockers application were (in sec) apamin : 1.54 ± 0.30 and 1.25 ± 0.26 (n = 12, p = 0.0342), paxilline : 1.34 ± 0.30 and 1.35 ± 0.28 (n = 8, p = 0.4688), TRAM 34 : 2.17 ± 0.19 and 1.91 ± 0.22 (n = 17, p = 0.0711). However, if we examine our data, we would find that after TRAM 34 application, only one cell had PSI duration increased. If we excluded this outlier, PSI durations before and after TRAM 34 would be (in sec) 2.16 ± 0.20 and 1.78 ± 0.19 (n = 16, p = 0.0007), representing that TRAM 34 could

doi:10.6342/NTU202203169

decrease PSI duration significantly. Since baseline activity also rose after TRAM 34 application (Fig.8 D3), it could also be the reason for PSI duration shortening. To sum up, the result shown that apamin and TRAM 34 could be able to decrease PSI duration.

3.5.3 Whole cell recoding with 0.1 mM EGTA internal

In cell-attach recording, due to being unable to control baseline activity by adjusting holding current, baseline activity could not be maintained at similar rate throughout PSI measurement. To re-check our result, we repeated the experiments using whole cell recording with 0.1 mM EGTA internal buffer (Fig.9 A). PSI durations before and after apamin and TRAM 34 application were (in sec) 2.00 ± 0.07 and 1.86 ± 0.07(n = 8, p = 0.0022), 2.12 ± 0.09 and 2.00 ± 0.08 (n = 9, p = 0.1304). As shown in Fig.9 B, PSI durations still decreased after apamin application. However, PSI durations were statistically unchanged after TRAM 34 application, suggesting that the reduction on PSI durations we observed in cell-attach recordings may be resulted from acceleration of baseline activity. Although burst activities were slightly increased following apamin and TRAM 34 application (Fig.9 C), according to Fig.11 B, the small changes in burst activity should not cause much difference in PSI duration.

doi:10.6342/NTU202203169

3.6 Effects of $GABA_b$ receptor on PSI : cgp54626 decrease PSI duration

To test whether GABAergic inhibitory interneurons would affect PSI duration, we applied 10 μM cgp54626 which is a $GABA_b$ receptor antagonist (Fig.10 A). As presented in Fig.10 B, PSI durations significantly decreased after cgp54626 application. PSI durations before and after cgp54626 application were (in sec) 2.45 ± 0.10 and 2.24 ± 0.09 ($n = 8$, $p < 0.0084$). Since baseline activity and burst frequency remained unchanged post cgp54626 application (Fig.10 C), effects on PSI duration should be independent of them.

Summary

In our experiments, we found that PSI duration was strongly dependent on baseline activity, and that Idazoxan (α_2-AR antagonist), apamin (SK channel blocker), cgp54626 ($GABA_b$ antagonist) could decrease PSI duration independent of baseline activity. Our results suggest that auto inhibition by α_2-AR antagonist and intrinsic property of LC neurons and local circuits are all involving in PSI duration modulation.

doi:10.6342/NTU202203169

Chapter 4. Discussion

4.1 Experimental limitations

In our experiments, we use ex-vivo acute brain slices and induce PSI by I-injection or optogenetic stimulation to study mechanism underlying PSI. However, due to experimental limitation, there could still be difference between PSI we recorded from in-vivo PSI.

4.1.1 Norepinephrine supply in acute slices

Studies upon LC α_2-AR have shown that α_2-AR antagonist could accelerate in-vivo recorded LC tonic activity, but have no effect on ex-vivo recorded tonic activity using acute brain slices. Since α_2-AR agonist application can still inhibit tonic activity in acute brain slices, and can be reversed by α_2-AR antagonist, α_2-AR should still be functional in acute brain slices (Aghajanian et al. 1982, Andrade et al. 1984). The effect could be caused by reduction of NE release due to removal of partial axons, dendrites and LC neurons while producing brain slices. According to the study, in vivo PSI should be different from PSI we recorded, and contribution of α_2-AR to PSI would also be different.

doi:10.6342/NTU202203169

4.1.2 Induced burst activity vs spontaneous phasic activity

In our experiments, burst activities were evoked by optogenetic stimulation or I-injection. As a result, PSI following evoked burst activity could differ from spontaneous phasic activity. Studies have shown that phasic-like activity could be found in LC neurons following medial prefrontal cortex (mPFC) stimulation (Jodo et al. 1997, 1998), indicating that mPFC could take part in generating LC phasic activity. Since mPFC also projects to peri-LC region (Lu, Yuefeng et al. 2012), where numerous inhibitory interneurons were reported (Aston-Jones et al. 2004). It is possible that while generating LC phasic activity, mPFC could also activate peri-LC inhibitory interneurons and contribute to PSI. This could also cause difference between ex-vivo PSI and in-vivo PSI. Similarly, brain regions related to LC phasic activity generating pathway could also cause difference between ex vivo PSI and in vivo PSI.

4.1.3 Optogenetic stimulation

In some of our experiments, we used light stimulations on channelrhodopsin2 (Chr2) expressed on LC neurons to evoke burst activities. However, not every LC neuron was capable of generating burst activity by light stimulation, which may result from Chr2 expression difference from neuron to neuron. As a result, the number and distribution of LC neurons that could generate burst activities together with the recorded LC neuron

doi:10.6342/NTU202203169

could vary from brain slices to slices. Therefore, if there were effects that required specific spatial relationship between recorded neuron and burst generating neurons (like close enough), I may not be able to observe it in every brain slice.

4.2 Inhibition between LC neurons

4.2.1 Efferent subpopulation of LC

Although LC has been thought to be homogeneous, recent studies have shown that LC could be divided into subpopulations by molecular markers or projection targets (Uematsu A et al. 2015, Schwarz et al. 2015, Plummer et al. 2020). These findings suggest that LC efferent subpopulation map could exist. Hence, if phasic causing input like novel, salient or task related stimuli could cause phasic activity in specific LC subpopulations, only NE input to corresponding brain regions would be activated. Therefore, by generating phasic activity in different subpopulations, a variety of effects could happen.

4.2.2 Lateral inhibition on non-phasic LC neurons

Antidromic stimulations uncapable of inducing burst activities on recorded LC neurons can still generate PSI, indicating that lateral inhibition between LC neurons should exist (Ennis et al. 1986). Our experiments also exhibit similar result. As

doi:10.6342/NTU202203169

mentioned before, not every LC neuron could generate burst activities post optogenetic stimulations. But PSI could still be observed in both LC neurons with or without burst activities (supplementary.2). Inhibition between LC neurons could be resulted from NE released into extracellular space, or through activation of local inhibitory interneurons. Although, according to our result, this inhibition should not affect PSI following burst activities (Fig.3). In theory, following phasic activity, LC neurons could cause inhibition on LC neurons that is not generating phasic activity together. The inhibition could lead to a drop in NE levels in corresponding brain regions without the presence of phasic activity, and may play parts in effects following phasic activity.

doi:10.6342/NTU202203169

Chapter 5. Reference

Aghajanian G. K. (1985). Modulation of a transient outward current in serotonergic neurones by alpha 1-adrenoceptors. Nature, 315(6019), 501–503.

Aghajanian, G. K., & VanderMaelen, C. P. (1982). alpha 2-adrenoceptor-mediated hyperpolarization of locus coeruleus neurons: intracellular studies in vivo. Science (New York, N.Y.), 215(4538), 1394–1396.

Aghajanian, G. K., Cedarbaum, J. M., & Wang, R. Y. (1977). Evidence for norepinephrine-mediated collateral inhibition of locus coeruleus neurons. Brain research, 136(3), 570–577.

Andrade, R., & Aghajanian, G. K. (1984). Locus coeruleus activity in vitro: intrinsic regulation by a calcium-dependent potassium conductance but not alpha 2-adrenoceptors. *The Journal of neuroscience : the official journal of the Society for Neuroscience*, *4*(1), 161–170.

Arima, J., Kubo, C., Ishibashi, H., & Akaike, N. (1998). alpha2-Adrenoceptor-mediated potassium currents in acutely dissociated rat locus coeruleus neurones. *The Journal of physiology*, *508 (Pt 1)*(Pt 1), 57–66.

Aston-Jones, G., & Bloom, F. E. (1981). Activity of norepinephrine-containing locus coeruleus neurons in behaving rats anticipates fluctuations in the sleep-waking cycle. *The Journal of neuroscience : the official journal of the Society for Neuroscience*, *1*(8), 876–886.

Aston-Jones, G., Rajkowski, J., Kubiak, P., & Alexinsky, T. (1994). Locus coeruleus neurons in monkey are selectively activated by attended cues in a vigilance task. *The Journal of neuroscience : the official journal of the Society for Neuroscience*, *14*(7), 4467–4480.

doi:10.6342/NTU202203169

Aston-Jones, G., Chiang, C., & Alexinsky, T. (1991). Discharge of noradrenergic locus coeruleus neurons in behaving rats and monkeys suggests a role in vigilance. *Progress in brain research*, *88*, 501–520.

Aston-Jones, G., Zhu, Y., & Card, J. P. (2004). Numerous GABAergic afferents to locus ceruleus in the pericerulear dendritic zone: possible interneuronal pool. *The Journal of neuroscience : the official journal of the Society for Neuroscience*, *24*(9), 2313–2321.

Aston-Jones, G., & Cohen, J. D. (2005). An integrative theory of locus coeruleus-norepinephrine function: adaptive gain and optimal performance. *Annual review of neuroscience*, *28*, 403–450.

Bouret, S., & Sara, S. J. (2004). Reward expectation, orientation of attention and locus coeruleus-medial frontal cortex interplay during learning. *The European journal of neuroscience*, *20*(3), 791–802.

Bouret, S., & Sara, S. J. (2005). Network reset: a simplified overarching theory of locus coeruleus noradrenaline function. *Trends in neurosciences*, *28*(11), 574–582.

Carter, Matthew E et al. (2010). Tuning arousal with optogenetic modulation of locus coeruleus neurons. *Nature neuroscience*, *13*(12), 1526–1533.

Cedarbaum, J. M., & Aghajanian, G. K. (1976). Noradrenergic neurons of the locus coeruleus: inhibition by epinephrine and activation by the alpha-antagonist piperoxane. *Brain research*, *112*(2), 413–419.

Chen, F. J., & Sara, S. J. (2007). Locus coeruleus activation by foot shock or electrical stimulation inhibits amygdala neurons. *Neuroscience*, *144*(2), 472–481.

doi:10.6342/NTU202203169

Clayton, E. C., Rajkowski, J., Cohen, J. D., & Aston-Jones, G. (2004). Phasic activation of monkey locus ceruleus neurons by simple decisions in a forced-choice task. *The Journal of neuroscience : the official journal of the Society for Neuroscience*, *24*(44), 9914–9920.

Duan X, Nagel G, Gao S. (2019) Mutated Channelrhodopsins with Increased Sodium and Calcium Permeability. *Applied Sciences*. 2019; 9(4):664.

Ennis, M., & Aston-Jones, G. (1986). Evidence for self- and neighbor-mediated postactivation inhibition of locus coeruleus neurons. *Brain research*, *374*(2), 299–305.

Foote, S. L., & Morrison, J. H. (1987). Extrathalamic modulation of cortical function. *Annual review of neuroscience*, *10*, 67–95.

Grella, Stephanie L et al. (2019). Locus Coeruleus Phasic, But Not Tonic, Activation Initiates Global Remapping in a Familiar Environment. *The Journal of neuroscience : the official journal of the Society for Neuroscience*, *39*(3), 445–455.

Huang, Hong-Ping et al. (2012). Physiology of quantal norepinephrine release from somatodendritic sites of neurons in locus coeruleus. *Frontiers in molecular neuroscience*, *5*, 29. https://doi.org/10.3389/fnmol.2012.00029

Jedema, Hank P et al. (2008). Chronic cold exposure increases RGS7 expression and decreases alpha(2)-autoreceptor-mediated inhibition of noradrenergic locus coeruleus neurons. *The European journal of neuroscience*, *27*(9), 2433–2443.

Jodo, E., Chiang, C., & Aston-Jones, G. (1998). Potent excitatory influence of prefrontal cortex activity on noradrenergic locus coeruleus neurons. *Neuroscience*, *83*(1), 63–79.

doi:10.6342/NTU202203169

Jodo, E., & Aston-Jones, G. (1997). Activation of locus coeruleus by prefrontal cortex is mediated by excitatory amino acid inputs. *Brain research*, *768*(1-2), 327–332.

Kawano, H., Mitchell, S. B., Koh, J. Y., Goodman, K. M., & Harata, N. C. (2020). Calcium-induced calcium release in noradrenergic neurons of the locus coeruleus. *Brain research*, *1729*, 146627.

Lu, Y., Simpson, K. L., Weaver, K. J., & Lin, R. C. (2012). Differential distribution patterns from medial prefrontal cortex and dorsal raphe to the locus coeruleus in rats. *Anatomical record (Hoboken, N.J. : 2007)*, *295*(7), 1192–1201.

Marzo, A., Bai, J., & Otani, S. (2009). Neuroplasticity regulation by noradrenaline in mammalian brain. *Current neuropharmacology*, *7*(4), 286–295.

Matschke, Lina A et al. (2015). A concerted action of L- and T-type Ca(2+) channels regulates locus coeruleus pacemaking. *Molecular and cellular neurosciences*, *68*, 293–302.

Matschke, L. A., Rinné, S., Snutch, T. P., Oertel, W. H., Dolga, A. M., & Decher, N. (2018). Calcium-activated SK potassium channels are key modulators of the pacemaker frequency in locus coeruleus neurons. *Molecular and cellular neurosciences*, *88*, 330–341.

Neves, R. M., van Keulen, S., Yang, M., Logothetis, N. K., & Eschenko, O. (2018). Locus coeruleus phasic discharge is essential for stimulus-induced gamma oscillations in the prefrontal cortex. *Journal of neurophysiology*, *119*(3), 904–920.

doi:10.6342/NTU202203169

Pieribone, V. A., Nicholas, A. P., Dagerlind, A., & Hökfelt, T. (1994). Distribution of alpha 1 adrenoceptors in rat brain revealed by in situ hybridization experiments utilizing subtype-specific probes. *The Journal of neuroscience : the official journal of the Society for Neuroscience*, *14*(7), 4252–4268.

Plummer, Nicholas W et al. (2020). An Intersectional Viral-Genetic Method for Fluorescent Tracing of Axon Collaterals Reveals Details of Noradrenergic Locus Coeruleus Structure. *eNeuro*, *7*(3), ENEURO.0010-20.2020.

Ramos, B. P., & Arnsten, A. F. (2007). Adrenergic pharmacology and cognition: focus on the prefrontal cortex. *Pharmacology & therapeutics*, *113*(3), 523–536.

Rajkowski, J., Majczynski, H., Clayton, E., & Aston-Jones, G. (2004). Activation of monkey locus coeruleus neurons varies with difficulty and performance in a target detection task. *Journal of neurophysiology*, *92*(1), 361–371.

Sah, P., & Faber, E. S. (2002). Channels underlying neuronal calcium-activated potassium currents. *Progress in neurobiology*, *66*(5), 345–353.

Schwarz, Lindsay A et al. (2015). Viral-genetic tracing of the input-output organization of a central noradrenaline circuit. *Nature*, *524*(7563), 88–92.

Scheinin, M et al. (1994). Distribution of alpha 2-adrenergic receptor subtype gene expression in rat brain. *Brain research. Molecular brain research*, *21*(1-2), 133–149.

Schwarz, L. A., & Luo, L. (2015). Organization of the locus coeruleus-norepinephrine system. *Current biology : CB*, *25*(21), R1051–R1056.

Séguéla, P., Watkins, K. C., Geffard, M., & Descarries, L. (1990). Noradrenaline axon terminals in adult rat neocortex: an immunocytochemical analysis in serial thin sections. *Neuroscience*, *35*(2), 249–264.

doi:10.6342/NTU202203169

Stocker, M., Hirzel, K., D'hoedt, D., & Pedarzani, P. (2004). Matching molecules to function: neuronal Ca2+-activated K+ channels and afterhyperpolarizations. *Toxicon : official journal of the International Society on Toxinology*, *43*(8), 933–949.

Timmons, S. D., Geisert, E., Stewart, A. E., Lorenzon, N. M., & Foehring, R. C. (2004). alpha2-Adrenergic receptor-mediated modulation of calcium current in neocortical pyramidal neurons. *Brain research*, *1014*(1-2), 184–196.

Ting, J. T., Daigle, T. L., Chen, Q., & Feng, G. (2014). Acute brain slice methods for adult and aging animals: application of targeted patch clamp analysis and optogenetics. *Methods in molecular biology (Clifton, N.J.)*, *1183*, 221–242.

Uematsu, A., Tan, B. Z., & Johansen, J. P. (2015). Projection specificity in heterogeneous locus coeruleus cell populations: implications for learning and memory. *Learning & memory (Cold Spring Harbor, N.Y.)*, *22*(9), 444–451.

Vazey, E. M., Moorman, D. E., & Aston-Jones, G. (2018). Phasic locus coeruleus activity regulates cortical encoding of salience information. *Proceedings of the National Academy of Sciences of the United States of America*, *115*(40), E9439–E9448.

Xiang, L., Harel, A., Gao, H., Pickering, A. E., Sara, S. J., & Wiener, S. I. (2019). Behavioral correlates of activity of optogenetically identified locus coeruleus noradrenergic neurons in rats performing T-maze tasks. *Scientific reports*, *9*(1), 1361.

Zhong, H., & Minneman, K. P. (1999). Alpha1-adrenoceptor subtypes. *European journal of pharmacology*, *375*(1-3), 261–276.

doi:10.6342/NTU202203169

Zhao, Y., Fang, Q., Straub, S. G., Lindau, M., & Sharp, G. W. (2010). Noradrenaline inhibits exocytosis via the G protein βγ subunit and refilling of the readily releasable granule pool via the α(i1/2) subunit. *The Journal of physiology*, *588*(Pt 18), 3485–3498.

doi:10.6342/NTU202203169

Chapter 6. Figures

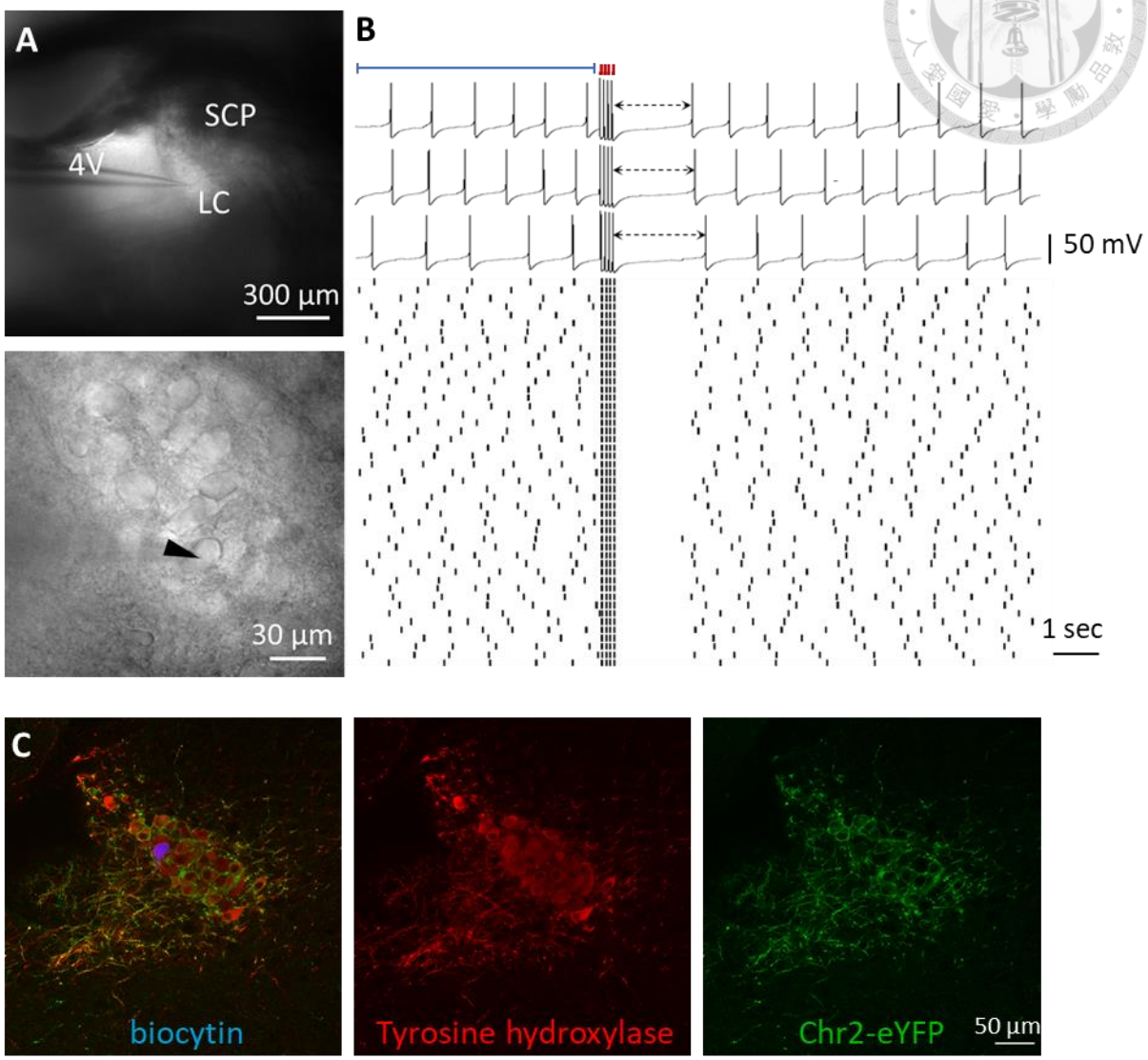

Fig 1. PSI duration testing set up.

A, DIC images of brain slice containing LC of 10x object lens (up) and 40x object lens (down). Triangle labeled recorded LC neuron. B, Example of PSI duration measurement. Red dots represent burst stimulation and blue line period represent baseline activity. Dashed lines represent PSI duration. C, Confocal image of post hoc validation. 4V : 4th ventricle, scp : superior cerebellar peduncles, LC : locus coeruleus.

doi:10.6342/NTU202203169

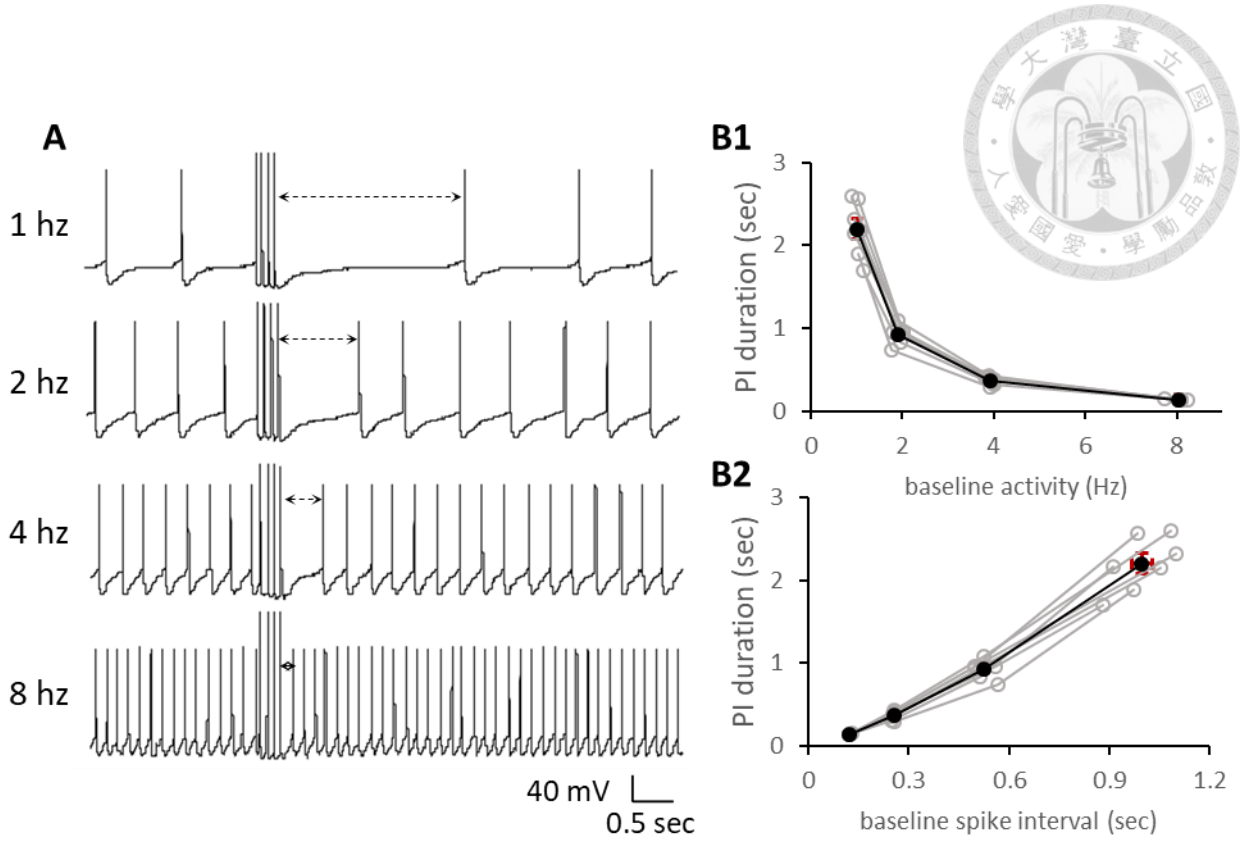

Fig 2. PSI duration under different baseline activity level

A, examples of I-injection induced PSI duration (dashed line) for 1, 2, 4 and 8 hz baseline activity. B1, baseline activity - PSI duration scatter plot. B2, baseline spike interval - PSI duration.

doi:10.6342/NTU202203169

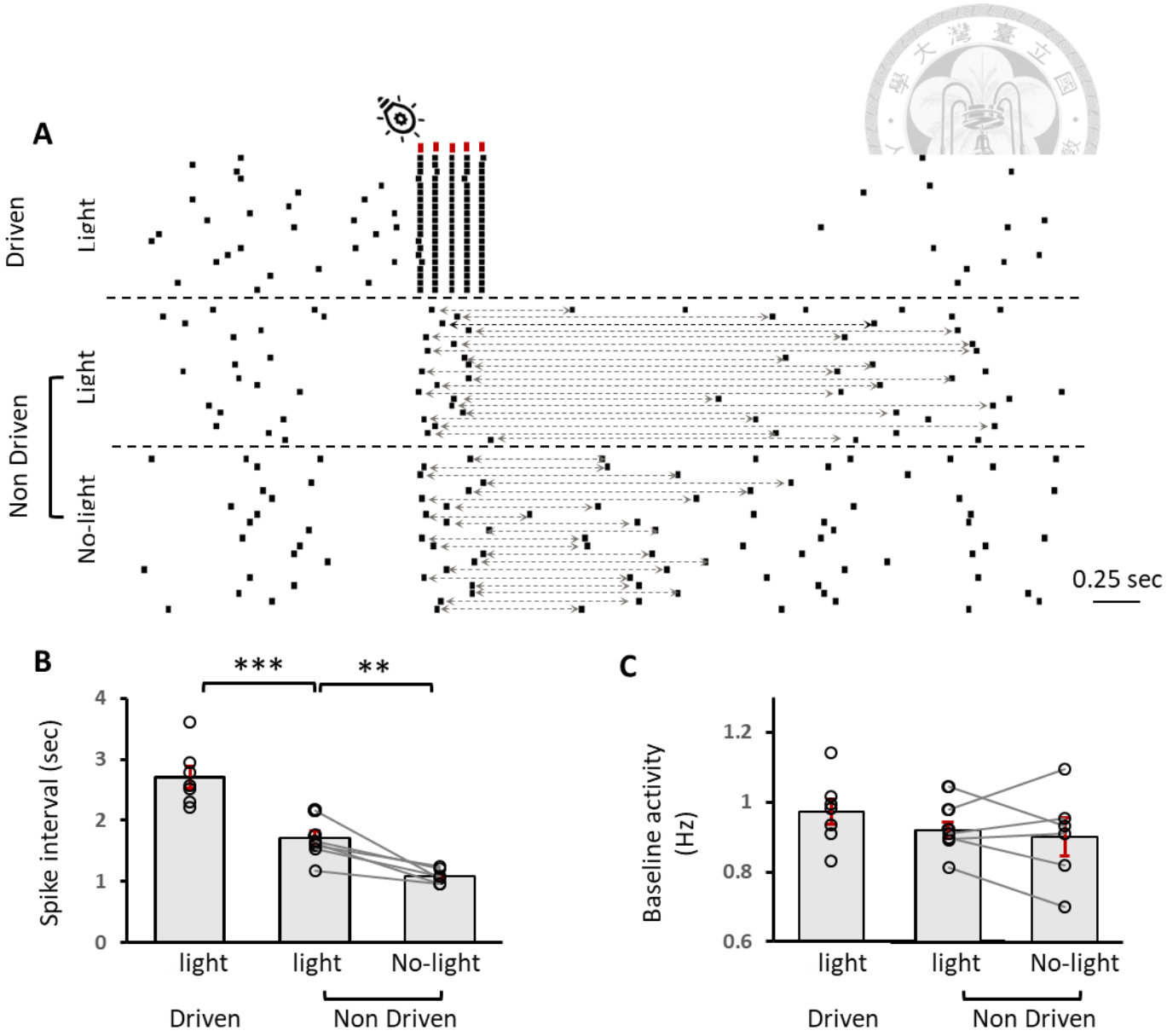

Fig. 3. Optogenetic stimulation on driven and non-driven neurons.

A, examples of trials whole-cell recording, red represent light stimulation to evoke burst activity. Dashed line represent PSI for no-driven. B.C, Spike interval (latency between last AP within stimulation period and the next spontaneous AP) and baseline activity for driven and non-driven neuron.

doi:10.6342/NTU202203169

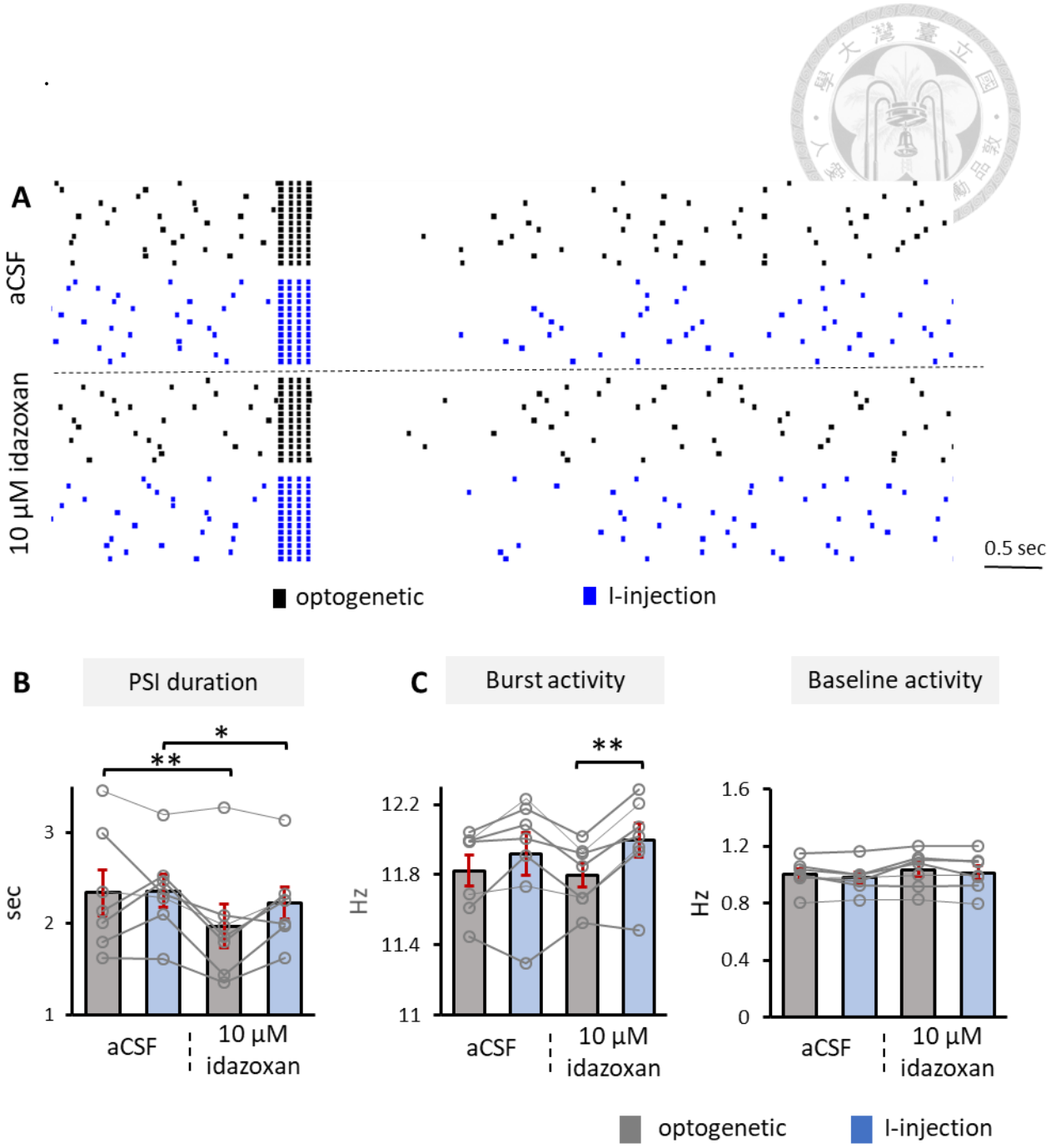

Fig 4. Effects of idazoxan on PSI of I-injection or optogenetic induced burst

A, examples of trials of recording before and after idazoxan application. Black represent burst induced by optogenetic stimulation, blue represents burst induced by I-injection. B,C, PSI duration, burst frequency and baseline activity before and after idazoxan application.

doi:10.6342/NTU202203169

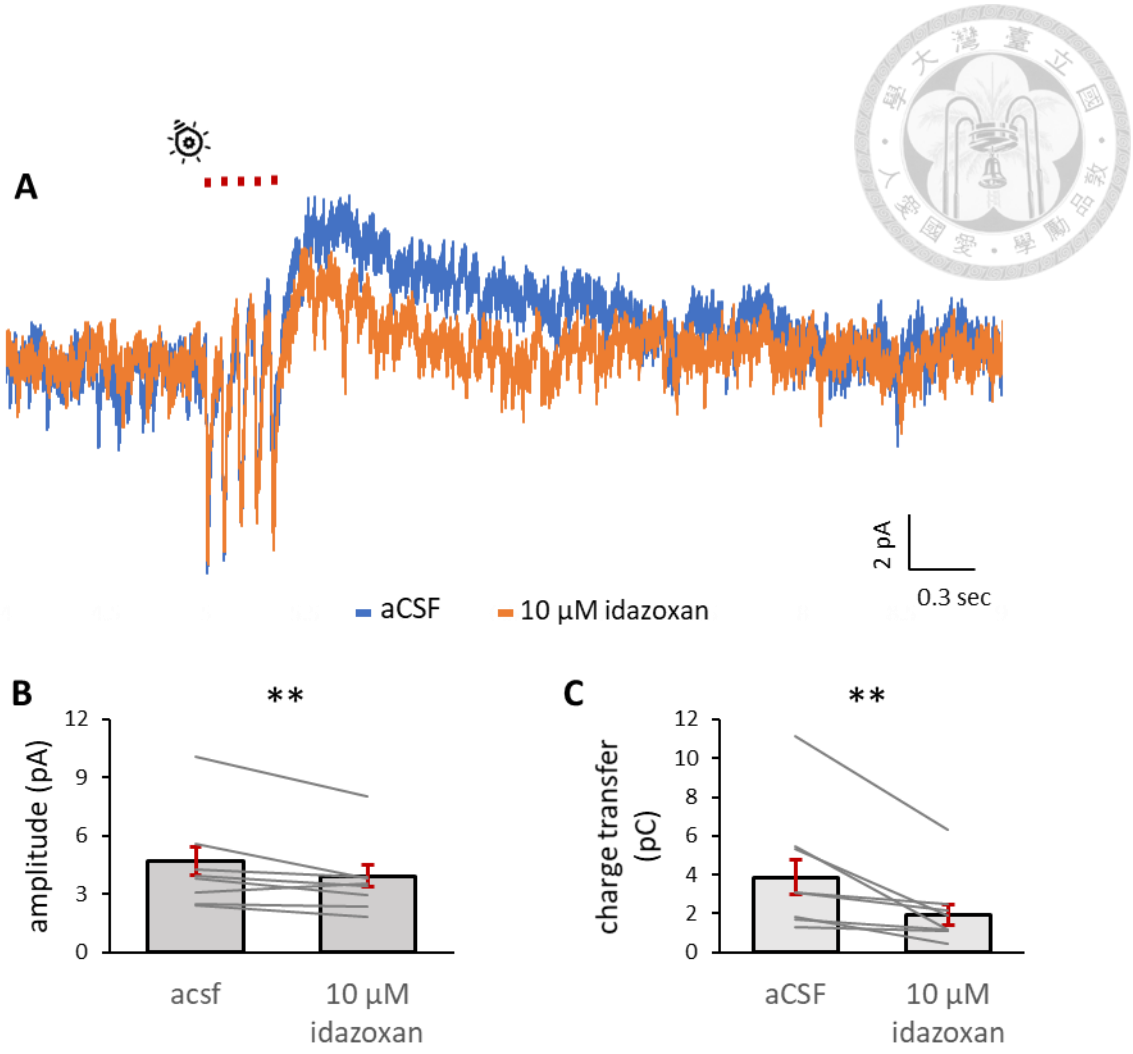

Fig 5. Outward current following optogenetic stimulation

A, An examples of average recording trace. B,D amplitude and charge transfer before and after idazoxan

doi:10.6342/NTU202203169

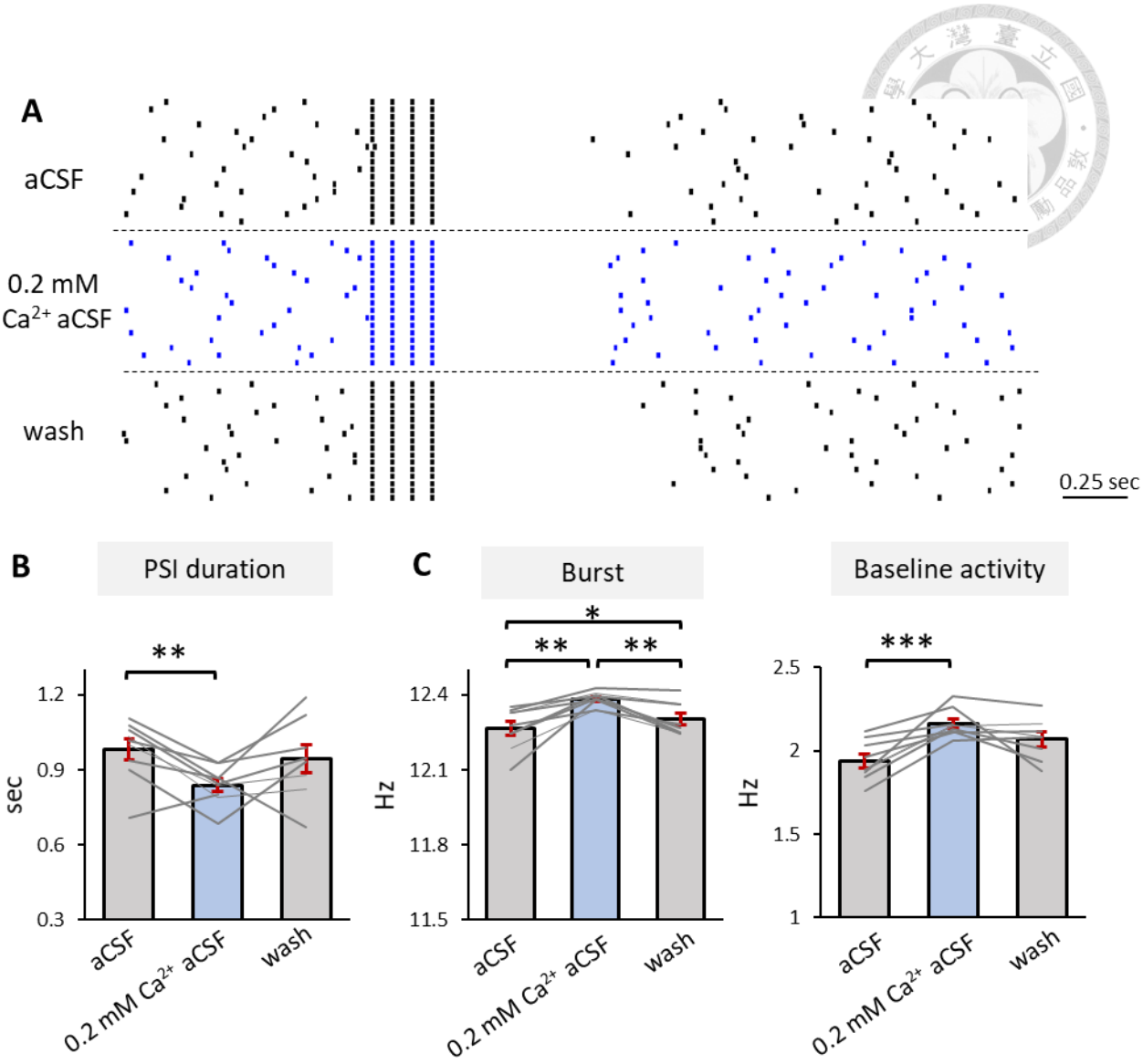

Fig 6. Effects of low aCSF Calcium concentration on PSI

A, examples of trials of recording in aCSF, 0.2 mM Ca^{2+}aCSF and wash with aCSF. Black represent perfusion solution is aCSF (Ca^{2+} 2.5 mM), and blue represent perfusion solution is 0.2 mM Ca^{2+}aCSF. B.C, PSI duration, burst and baseline activity in aCSF, 0.2 mM Ca^{2+}aCSF, and wash.

doi:10.6342/NTU202203169

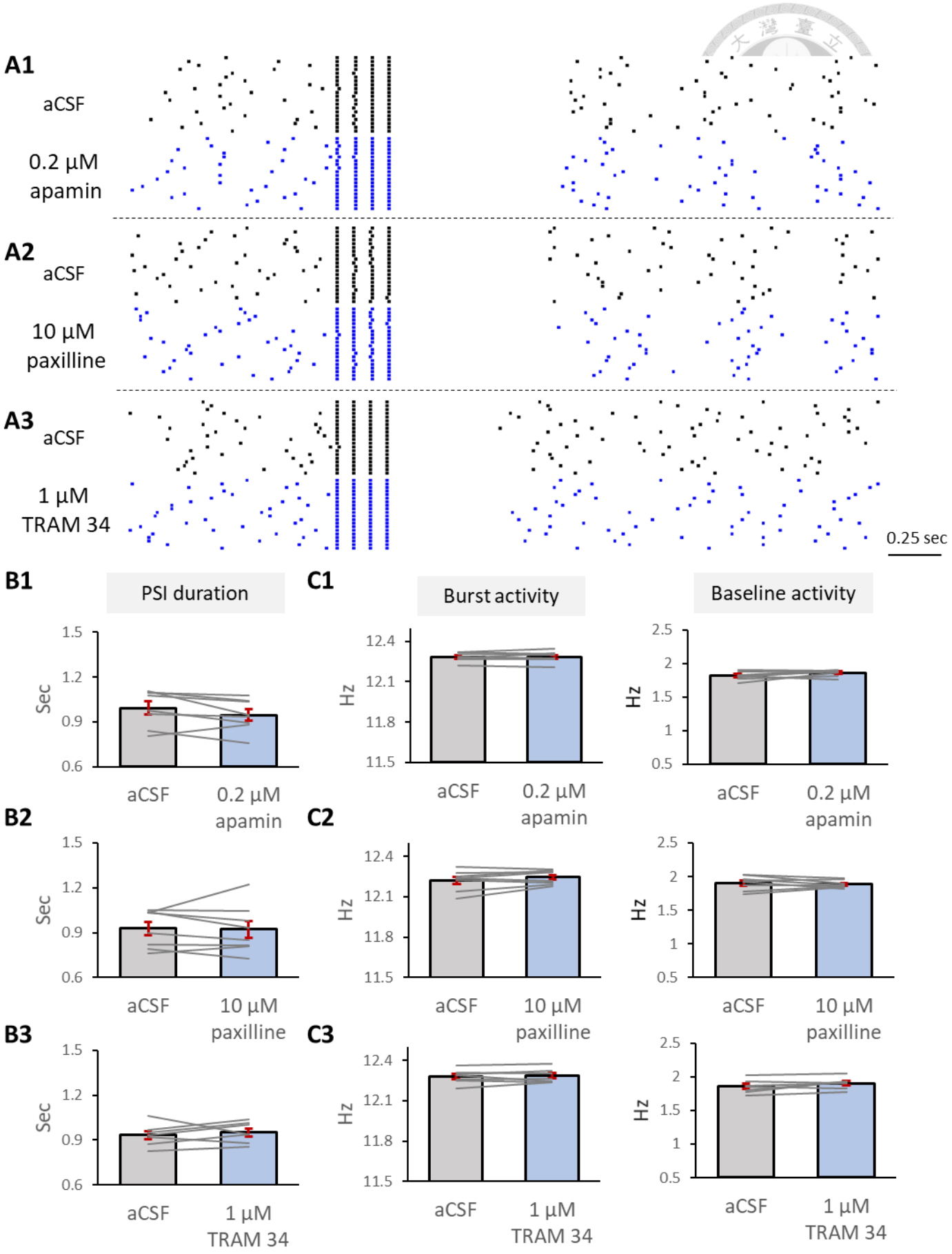

doi:10.6342/NTU202203169

Fig 7. Effects of K_{Ca} channel blockers on PSI

A, examples of trials of whole-cell recording under treatments. Black represents before blockers application, and blue represents K_{Ca} channel blockers (apamin (SK blocker), paxilline (BK blocker) or TRAM 34 (IK blocker)) have been applied. B.C, PSI duration, burst and baseline activity before and after K_{Ca} channel blocker treatments.

doi:10.6342/NTU202203169

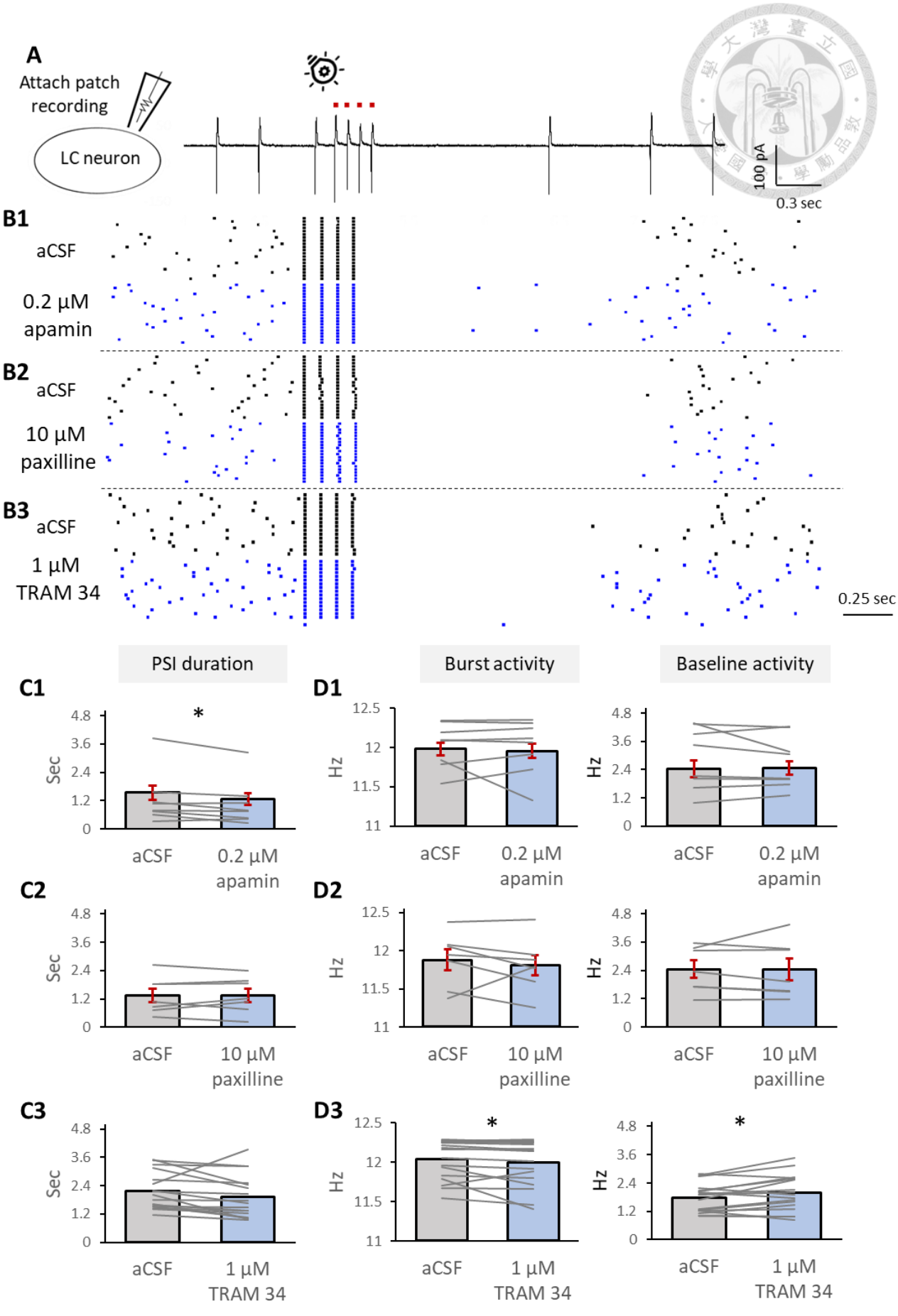

doi:10.6342/NTU202203169

Fig 8. Effects of K_{Ca} channel blockers on PSI (cell-attach recording)

A, a diagram of cell-attach recording, and a trial of recording contain optogenetic induced burst. B , a example of trials of recording. Black represents before drug application, and blue represents K_{Ca} channel blockers (apamin (SK blocker), paxilline (BK blocker) or TRAM 34 (IK blocker)) have been applied. B.C, PSI duration, burst and baseline activity frequency before and after treatments.

doi:10.6342/NTU202203169

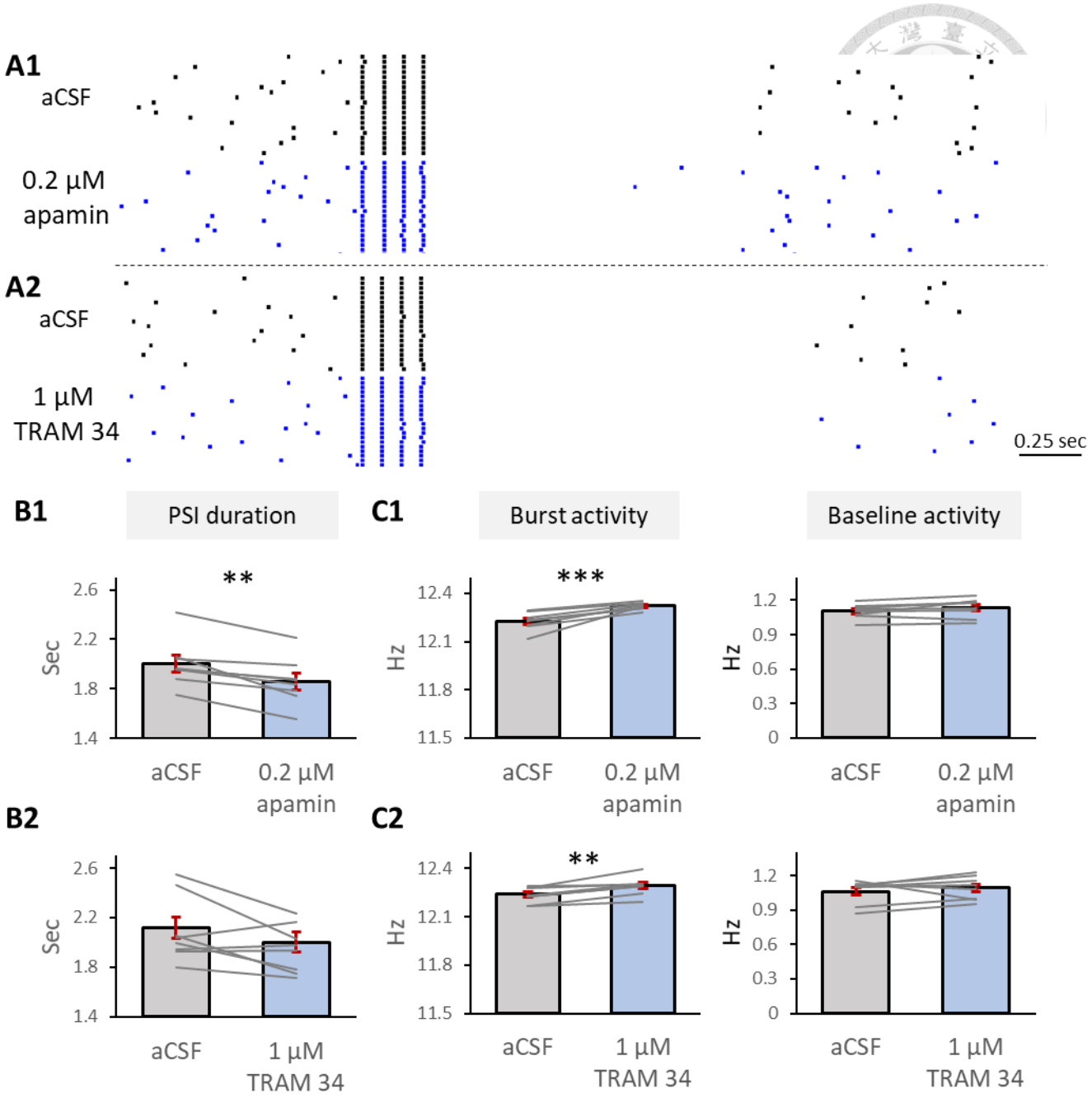

Fig 9. Effects of K_{Ca} channel blockers on PSI (low EGTA)

A, examples of trials of recording. Black represents before drug application, and blue represents K_{Ca} channel blockers (apamin (SK blocker) or TRAM 34 (IK blocker)) have been applied. Burst was induced by I-injection. B.C, PSI duration, burst and baseline activity before and after treatments.

doi:10.6342/NTU202203169

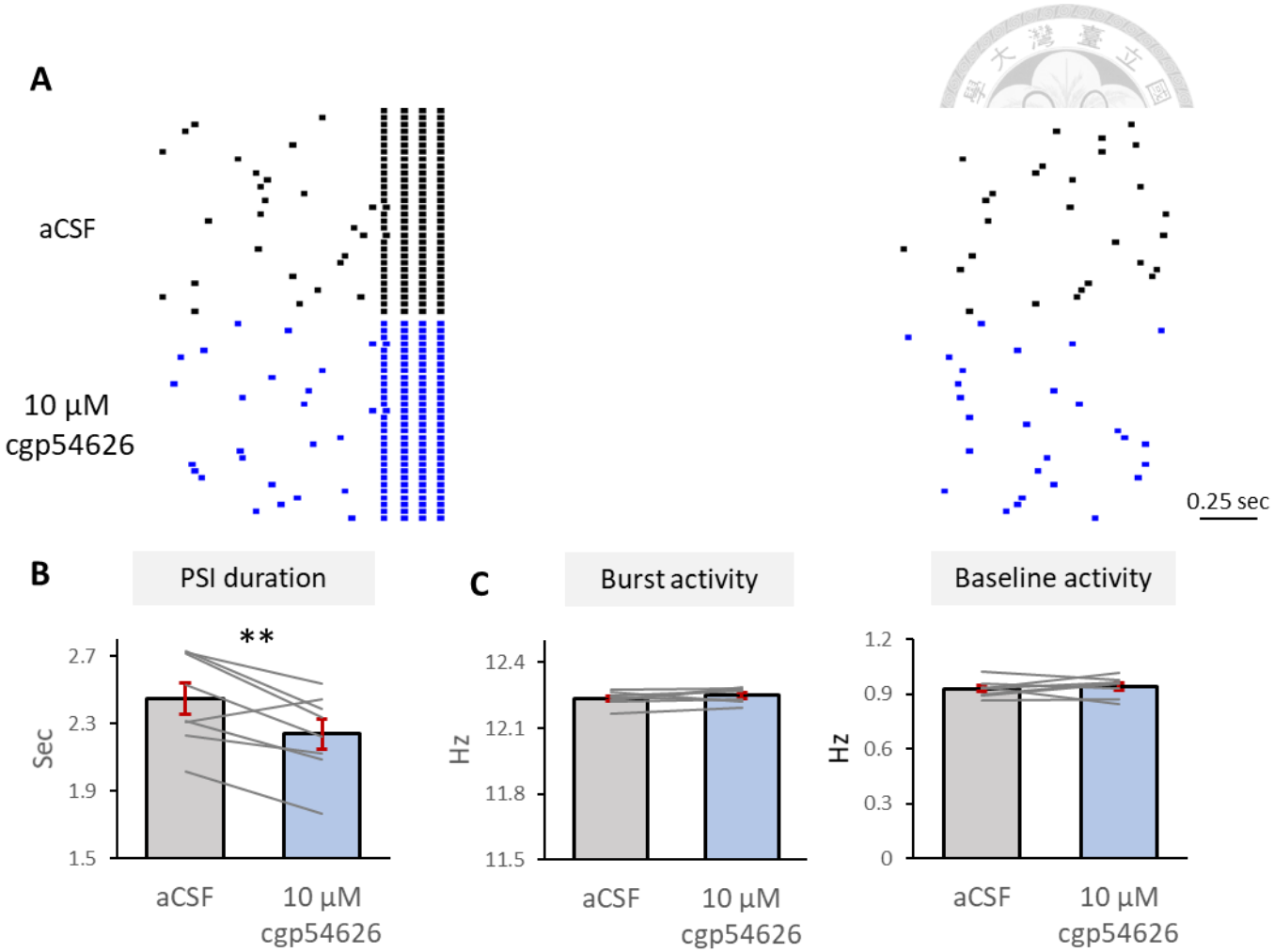

Fig 10. Effects of $GABA_b$ blocker on PSI

A, examples of trials whole-cell recording. Black represents perfusion is with pure aCSF, and blue represents $GABA_b$ clocker cgp54626 have been applied. Burst was induced by I-injection. B.C, PSI duration, burst and baseline activity before and after treatments.

doi:10.6342/NTU202203169

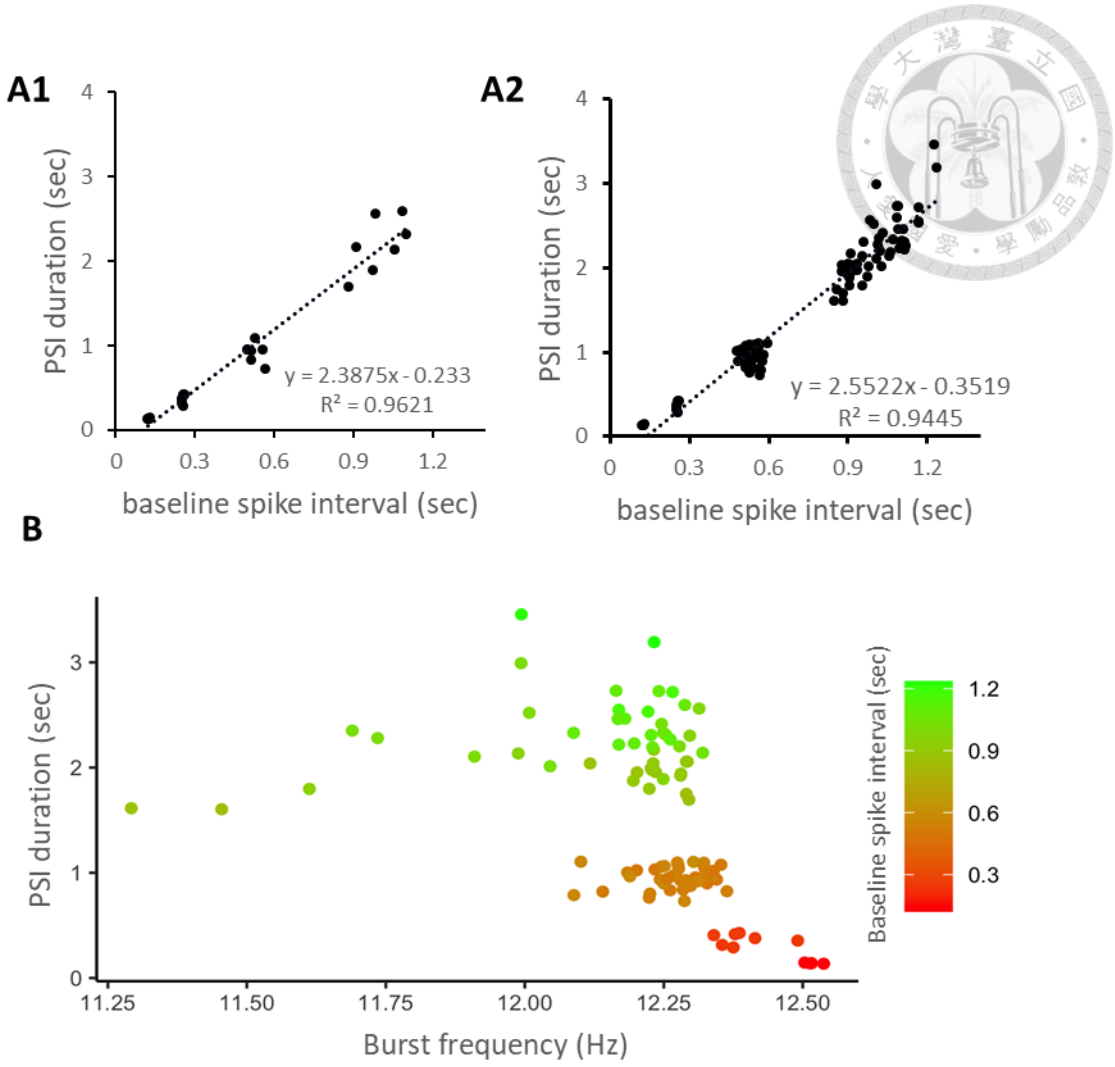

Fig 11. Correlation of PSI duration with baseline activity and burst activity

A, baseline spike interval – PSI duration scatter plot, A1 : data of Fig 2, A2 : data of all whole-cell clamp experiments before treatments . B, burst frequency – PSI duration (color represent baseline spike interval).

doi:10.6342/NTU202203169